

The invariance of directional tuning with contrast and coherence

I. Fine^{a,*}, C.M. Anderson^a, G.M. Boynton^b, K.R. Dobkins^a

^a Department of Psychology, UC San Diego, La Jolla, CA, USA

^b The SALK Institute, La Jolla, CA, USA

Received 19 August 2003; received in revised form 19 November 2003

Abstract

The responses of motion mechanisms depend not only on the direction of a stimulus, but also on its contrast, coherence and speed. We examined how contrast, coherence and directional selectivity interact by measuring directional tuning psychophysically across a wide range of coherence and contrast levels. We fit data with a simple model that estimated directional tuning bandwidth using contrast and coherence gain parameters that were based on neurophysiological estimates. This model estimated a bandwidth of $\sim 90^\circ$ for directionally selective mechanisms. Bandwidth was invariant across a wide range of contrasts and coherences, as predicted by models of contrast normalization.

© 2004 Elsevier Ltd. All rights reserved.

1. Introduction

Several previous psychophysical and neurophysiological studies have investigated the directional selectivity of motion mechanisms by measuring tuning bandwidths. Psychophysical studies typically report bandwidths (width at half-height) ranging from 70° – 120° as determined from masking (Ball & Sekuler, 1979), uncertainty (Ball & Sekuler, 1980) and adaptation (Levinson & Sekuler, 1980; Raymond, 1993) experiments. Neurophysiological studies report similar bandwidths for direction-selective neurons in motion-sensitive brain areas of macaque monkeys, for example in area MT (Albright, 1984; Dubner & Zeki, 1971; Felleman & Kaas, 1984). However the responses of motion mechanisms do not simply depend on the direction of a moving stimulus, but also on its contrast, coherence and speed. Here we examine whether or not direction tuning is invariant with contrast and coherence.

Although no single study has directly measured tuning bandwidth as a function of contrast, a comparison

of data across psychophysical studies (using widely different stimulus parameters) suggests that tuning may change with increasing contrast. For example, psychophysical experiments measuring coherence thresholds with low contrast stimuli (Ball, Sekuler, & Machamer, 1983; Levinson & Sekuler, 1980) report bandwidths around 120° , while experiments employing high contrast stimuli report tuning around 80° (Raymond, 1993). Curiously, a study by Georgeson and Scott-Samuel (Georgeson & Scott-Samuel, 2000) inferring direction tuning indirectly through measuring receptive field length makes the opposite prediction. They found that receptive field heights decrease with contrast (up to contrasts of 20–40%). For a *linear* filter, receptive field length and direction bandwidth would be inversely related; the authors therefore suggest a possible increase in direction bandwidth with contrast. While no neurophysiological study has examined direction tuning as a function of stimulus contrast, the effects of contrast has been measured for orientation tuning, with results demonstrating invariance of orientation tuning across a wide range of contrasts (Sclar & Freeman, 1982; Skottun, Bradley, Sclar, Ohzawa, & Freeman, 1987).

With respect to stimulus coherence, a recent neurophysiological study found that the directional tuning of MT neurons is invariant for coherences ranging between 12% and 100%, with a bandwidth $\sim 80^\circ$ (Britten & Newsome, 1998). Directional tuning as a function of coherence has not yet been measured psychophysically.

* Corresponding author. Address: Doheny Retina Institute, Keck School of Medicine, USC, 1450 San Pablo Street, DEI 3605, Los Angeles, CA 90033, USA. Tel.: +1-8589454793; fax: +1-3234426766.

E-mail address: ifine@dohenyeyeinstitute.org (I. Fine).

In the present study, we used psychophysical techniques to measure the tuning bandwidths of motion mechanisms across a range of stimulus contrasts and coherences. We used a summation paradigm in which we measured thresholds for discriminating global motion from noise as a function of the difference in direction of motion between two overlapping fields of dots (Graham, 1989; Meese & Harris, 2001). We used a simple model to estimate bandwidth based on the assumption that the amount of summation between two superimposed fields of moving dots is a function of the angular difference between the two fields. This model describes our results well, and yields an estimated bandwidth for directionally selective mechanisms of roughly 90° that was nearly invariant across both contrast and coherence.

2. Methods

2.1. Subjects

One author and two undergraduate students served as observers for all conditions tested. All had normal, or corrected-to-normal, visual acuity. Except for the author (CMA) all observers were naïve to the purpose of the experiment.

2.2. Visual apparatus and stimuli

Stimuli consisted of 141 moving dots placed within a $7^\circ \times 7^\circ$ square aperture presented on a cathode ray tube (CRT) display (SONY Trinitron Multiscan 500PS) driven by a VSG board (Cambridge Research Systems) within a PC. Each dot subtended 0.16° , resulting in a dot density of 2.9 dots per square degree of visual angle. Background luminance was 10 cd/m^2 . Dot contrast and coherence differed with condition.

Stimuli were presented at a frame rate of 53.3 Hz. Each dot started in a random location within the aperture and then moved in a single direction for 3 frames, or 56.3 ms, which is referred to as the “dot lifetime”. The dot then disappeared and reappeared at a new position. If a dot’s path extended beyond the aperture within its lifetime it was randomly replaced somewhere within the aperture as a new dot. Each dot moved 0.21° on each frame. At our frame rate of 53.33 Hz, this created a dot velocity of $11^\circ/\text{s}$.

A two-interval forced-choice (2IFC) procedure was used, in which subjects reported which of two intervals contained a coherent global motion signal. The “signal” interval contained two fields of coherently moving dots as well as noise dots moving in random directions (see Fig. 1). The “noise” interval contained only randomly moving dots. The number of dots was always equal between noise and signal intervals. Both signal and noise

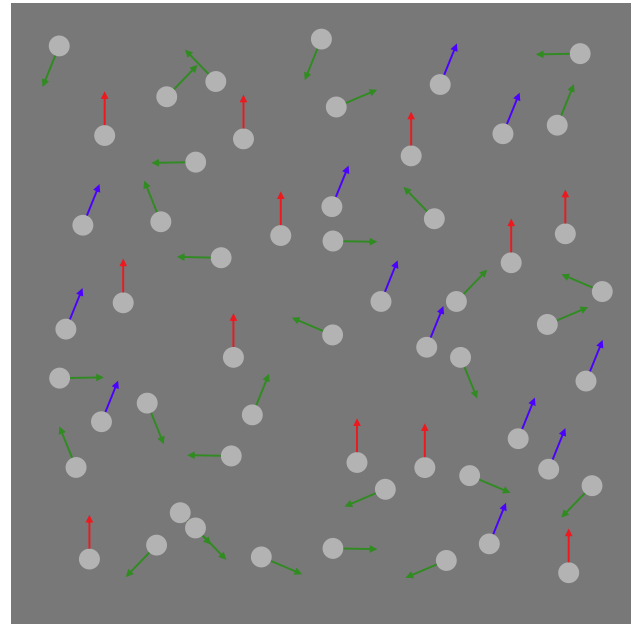


Fig. 1. Schematic representation of the signal stimulus. A 45% coherence, 3% contrast condition where $\delta = 22.5^\circ$. 22.5% of the dots moved upward (red arrows), 22.5% of the dots moved 22.5° clockwise from vertical (blue arrows) and the remaining 65% of the dots moved in random directions (green arrows).

dots were sampled from a distribution of 16 evenly spaced possible directions ($0^\circ, 22.5^\circ, 45^\circ, 67.5^\circ, 90^\circ, 112.5^\circ, 135^\circ, 157.5^\circ, 180^\circ, 202.5^\circ, 225^\circ, 247.5^\circ, 270^\circ, 292.5^\circ, 315^\circ, 337.5^\circ$).

In the signal interval, the angular difference between the two coherent fields of dots, δ , ranged between 0° (both fields moving in the same direction) to 180° (the two fields moving in opposite directions). There were 7 possible angular differences between the two fields: $\delta = 0^\circ, 22.5^\circ, 45^\circ, 67.5^\circ, 90^\circ, 135^\circ, \text{ and } 180^\circ$.

The coherence of the dots (i.e. the percentage of dots moving coherently vs. randomly in the ‘signal’ interval) was varied in our experiments, for the purpose of (1) obtaining coherent motion thresholds for a fixed contrast condition and (2) obtaining contrast thresholds for a fixed coherence condition (see below). We defined coherence as follows: a signal interval containing 20% coherence consisted of 10% of dots moving coherently in one direction, 10% moving in a second direction, and 80% moving randomly.

Note that both signal and noise dots traveled along a single path throughout their entire lifetime. We expect that results would have been similar if signal dots had traveled a variable path with a set displacement (Watanianuk, Sekuler, & Williams, 1989), or if we had used other types of noise dots, such as noise dots re-plotted in random positions in each new frame, or noise dots following a random walk from frame to frame (Scase, Braddick, & Raymond, 1996).

2.3. Procedure

Observers viewed the monitor binocularly using a chin rest at a distance of 52 cm. The height of the monitor was set so that the center of the aperture was approximately at eye level. Each trial began with observers fixating on a central fixation spot. Observers then pressed a key to begin each trial. Each trial consisted of two 300 ms intervals separated by a 400 ms interstimulus interval. Observers pressed a key reporting which interval contained coherent global motion. This motion tended to appear as either motion in a single direction, or as the transparent motion of two fields moving in different directions. Feedback was provided on each trial, with a tone signaling a correct response.

2.4. Varying contrast and coherence

The effects of contrast and coherence were measured in two ways: (1) *Fixed-contrast coherence-thresholds* were obtained. Dot contrast was kept fixed throughout a block of trials, and coherence was varied across trials (method of constant stimuli) to obtain coherence thresholds. Dot contrast is described in terms of rms contrast (Kukkonen, Rovamo, Tiippana, & Nasanen, 1993; Moulden, Kingdom, & Gatley, 1990) since this metric is thought to be the most appropriate for random dot patterns where dot density is low. Stimuli were presented at one of several fixed contrasts, spanning the range between 2.4% and 30% contrast. Each observer carried out four to six fixed contrast conditions. The entire set of rms contrasts used across all observers was 2.4%, 3.4%, 6.5%, 11%, 20% and 30%. Because we measured thresholds across 2 tasks and 16 direction differences for both a contrast and a coherence task, testing the complete set of coherences and contrasts for every subject would have required a prohibitive number of trials. Each observer therefore only performed the experiment for a subset of these fixed contrasts. The set of rms contrasts presented to all subjects were 3.4%, 6.5%, 11%, and 30%. As it was, each of our three subjects ended up performing more than 25,000 trials. Note that under some conditions/contrasts it was very difficult to obtain reliable thresholds, e.g. for the very low contrast conditions thresholds often could only be obtained for small values of δ .

(2) *Fixed-coherence contrast-thresholds* were obtained. Coherence was kept fixed throughout a block of trials, and contrast varied across trials to obtain contrast thresholds. Stimuli were presented at one of several fixed coherences spanning the range between 15% and 100% coherence (15%, 20%, 30%, 45%, 67% and 100%). Again, a subset of coherences (20%, 30%, 45% and 100%) was presented to all observers. Note that in the 100% coherence display each of the coherent motion

fields contained half the dots in the display and there were no noise dots.

We varied the contrast of the dots by changing their luminance, while keeping the mean background of the display at 10 cd/m². Contrast and the mean luminance of the display were therefore perfectly confounded. One approach would have been to use half black/half white dots (Morrone, Burr, & Vaina, 1995). However, because dot density was relatively low, the effect of dot contrast on the mean luminance of the display was relatively small. When the dots were at 2.4% contrast the mean luminance of the display was 10.1 cd/m², whereas when the dots were at 30% contrast the mean luminance of the display only increased to 11.4 cd/m².

Thus, while subjects were always performing the same task (which interval contained global motion) we obtained both coherence and contrast thresholds for each subject across a wide range of dot coherence and contrasts.

2.5. Data analysis

Each session contained 672 trials. Within each session the signal dots moved in each of the 16 possible directions an equal number of times and each angular separation (δ) was presented an equal number of times. Each subject carried out 5 sessions for each of the *fixed-contrast/coherence-threshold* and *fixed-coherence/contrast-threshold* conditions, resulting in a total of 40–55 sessions per subject (26,880–36,960 trials).

Data were averaged across each of the 16 possible directions, since analysis of the data revealed that performance was isotropic across all directions tested (Ball & Sekuler, 1979; Raymond, 1994; van Hateren, 1990). Weibull functions (480 trials per function, 80 trials per data point) were fit to the data using a maximum likelihood procedure for each angular separation, δ , in order to obtain 75% correct thresholds for all of the eight to twelve fixed conditions. Approximately 28 coherence thresholds and 28 contrast thresholds were obtained for each subject. It should be noted that using a Weibull function may not have been strictly appropriate for describing our data. As can be inferred from Fig. 5 below, for certain combinations of contrast and coherence performance asymptotes below 100%, while the Weibull function we used is constrained to (eventually) reach 100% performance. However, our goal was simply to interpolate to find the contrast and coherence at which observers performed at 75% correct. In practice we found that a Weibull function served our purpose well.

As described below, we fit our data with a model where we assumed that bandwidth could be inferred from the summation between the two fields of dots. We assumed that there would be a large amount of summation between the two dot fields when the directional difference between the two fields (δ) was small compared

to the directional bandwidth of the mechanisms responsible for detecting coherent motion. A similar summation paradigm has been used to calculate bandwidths for complex motion mechanisms (Meese & Harris, 2001).

3. Results

Example data from one subject (author CMA) fitted with Weibull functions are shown in Fig. 2, separately for a fixed-coherence condition (15% coherence, *panel A*, *solid symbols*) and a fixed-contrast condition (6.5% contrast, *panel B*, *open symbols*). Data are shown for the case where $\delta = 0^\circ$. In this example, a fixed-coherence of

15% yielded a contrast threshold of 5.1% contrast (*panel A*) while a fixed-contrast of 6.5% yielded a coherence threshold of 11.5%. Thresholds are the same regardless of whether coherence or contrast is fixed.

This is further revealed, in Fig. 2C, by plotting both the fixed-coherence and fixed-contrast data in terms of 75% iso-performance values, where the *x*-axis represents coherence and the *y*-axis represents contrast. Each point represents a particular conjunction of contrast and coherence that resulted in 75% correct performance. The filled symbols represent data collected using the *fixed-coherence* paradigm and the open symbols represent data collected using the *fixed-contrast* paradigm. Starred symbols represent the 75% thresholds from Fig. 2A and B. Filled and open symbols fall along the same curve,

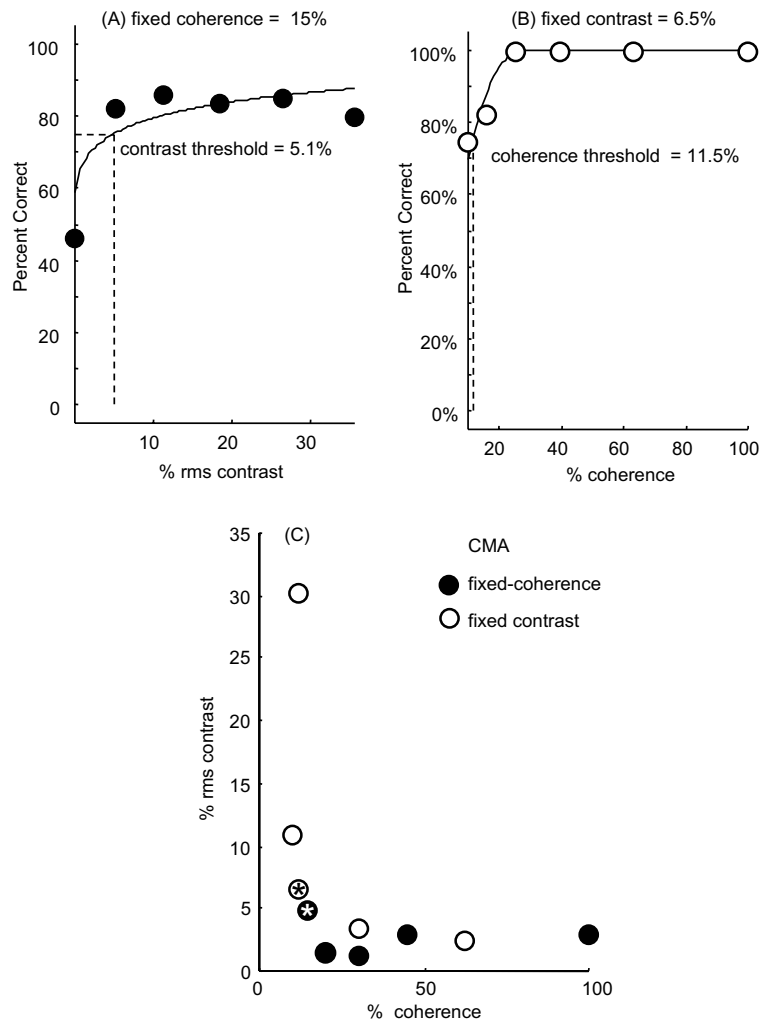


Fig. 2. (A) Weibull functions for subject CMA for $\delta = 0^\circ$. (A) Coherence was fixed at 15% and contrast was varied to find the 75% correct performance threshold. Contrast values are shown along the *x*-axis and percent correct is plotted along the *y*-axis. (B) Contrast was fixed at 6.5% and coherence was varied to find the 75% correct performance threshold. Coherence is plotted along the *x*-axis and percent correct is plotted along the *y*-axis. (C) Shows an iso-performance plot for $\delta = 0^\circ$ for CMA. The *x*-axis represents coherence and the *y*-axis represents contrast. Each point represents the particular conjunction of contrast and coherence that resulted in 75% correct performance. The filled symbols represent data collected using the *fixed-coherence* paradigm and the open symbols represent data collected using the *fixed-contrast* paradigm. Starred symbols represent thresholds from (A) and (B).

indicating that thresholds are unaffected by whether coherence is fixed and contrast varied, or vice versa.

Iso-performance curves are plotted for all 3 subjects in Fig. 3, separately for each of the seven angular separations between the two dot fields ($\delta = 0^\circ, 22.5^\circ, 45^\circ, 67.5^\circ, 90^\circ, 135^\circ, \text{ and } 180^\circ$). Data from the fixed-coherence condition are plotted with solid symbols, while data from the fixed-contrast condition are plotted with open symbols. Like the example data plotted in Fig. 2, these group data demonstrate that thresholds are the same regardless of whether coherence is fixed and contrast varied, or vice versa.

These group data also demonstrate that, at intermediate coherences and contrast values, there is a tradeoff between contrast and coherence. That is, increasing the contrast lowers the coherence needed to reach performance threshold, and vice versa. However, performance asymptotes along both axes. There are two possible reasons for these asymptotes. One explanation for the asymptote along the x -axis is that at very low contrasts, (below 2–3%) observers have difficulty detecting the

presence of the dots, regardless of their motion coherence. Alternatively, mechanisms may begin to saturate in their sensitivity to coherence for coherence values above $\sim 50\%$. Analogously, the asymptote along the y -axis might either be due to it being impossible to detect coherent motion for extremely low coherences, regardless of the contrast of the dots, or to saturation in the contrast-response function of motion mechanisms.

4. The model

To estimate directional-tuning bandwidth from this type of summation paradigm it is necessary to make assumptions about various parameters such as the shape of the contrast-response function, the coherence-response function, probability summation across mechanisms, and interactions between mechanisms (Meese & Harris, 2001). We chose to fit our data with a very simple model where we assumed that detection is mediated by mechanisms tuned to one of the two

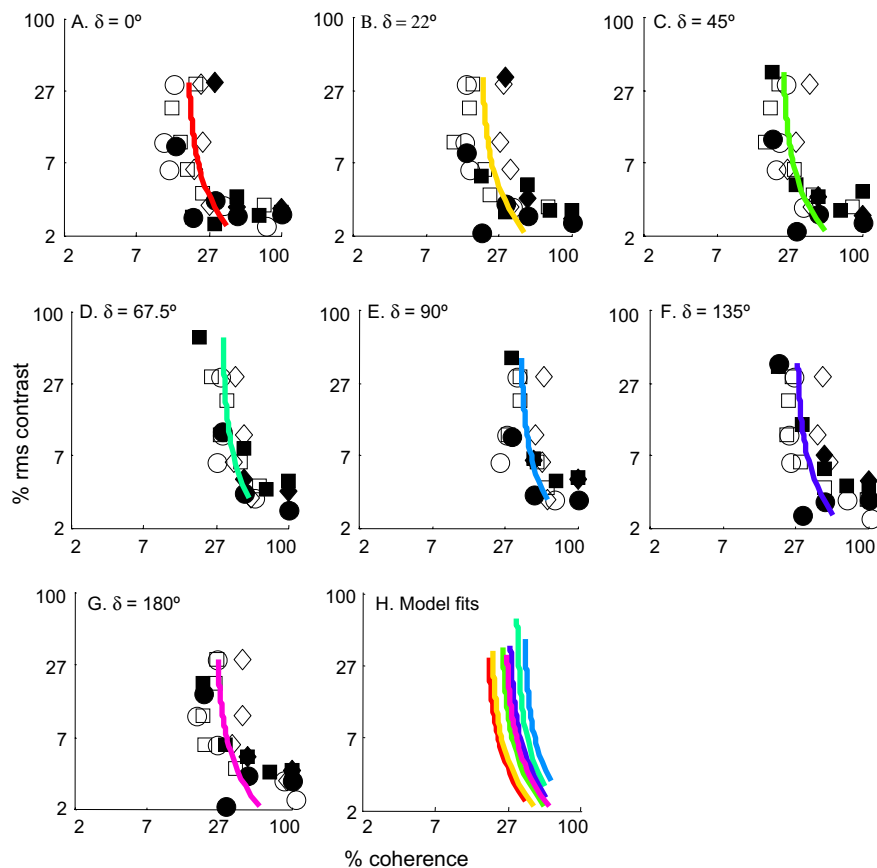


Fig. 3. (A)–(G) Iso-performance plots (75% correct) for various values of δ for all three subjects. The x -axis represents log coherence and the y -axis represents log contrast. Each point represents the particular conjunction of contrast and coherence that resulted in 75% correct performance. The filled symbols represent data collected using the *fixed-coherence* paradigm and the open symbols represent data collected using the *fixed-contrast* paradigm. Each subject is represented using a different symbol. The fits from our model are shown using colored curves. (H) The shape of the model fit remains constant, and each curve is simply shifted towards or away from the origin.

directions of coherent motion in the signal stimulus. The response of such a mechanism is:

$$R = h^q \frac{(c^{p_1+p_2})}{(c^{p_2} + \sigma^{p_2})} + wh^q \frac{(c^{p_1+p_2})}{(c^{p_2} + \sigma^{p_2})} \quad (1)$$

where c is the contrast of the dots, $\frac{(c^{p_1+p_2})}{(c^{p_2} + \sigma^{p_2})}$ describes contrast gain—how the response of the mechanism increases with increasing contrast in the stimulus, h is the coherence of the stimulus, q describes coherence gain—how the response of the mechanism increases with increasing coherence in the stimulus, w describes the relative sensitivity of the detecting mechanism to the second field of dots.

Thus, the first term, $h^q \frac{(c^{p_1+p_2})}{(c^{p_2} + \sigma^{p_2})}$, describes the response of the mechanism to a field of dots moving in the direction to which the mechanism is tuned. The second term, $wh^q \frac{(c^{p_1+p_2})}{(c^{p_2} + \sigma^{p_2})}$, is the response of the mechanism to the second field of coherently moving dots that is separated in motion direction by the angle δ . If the two fields travel in the same direction then $w = 1$. If the detecting mechanism is completely insensitive to the second field of dots then $w = 0$. If the second field of dots inhibits the response to the detecting mechanism then $w < 0$.

Eq. (1) can be reorganized as:

$$R = (w + 1)h^q \frac{(c^{p_1+p_2})}{(c^{p_2} + \sigma^{p_2})} \quad (2)$$

We further assumed that at a given magnitude of response $R = r$ the mechanisms mediating performance have a signal to noise ratio that produces a fixed threshold of performance (in terms of percent correct). This allows us to rearrange Eq. (2). For a given performance threshold we can predict the coherence needed to reach that threshold as a function of dot contrast.

$$h = \left[\frac{r(c^{p_2} + \sigma^{p_2})}{(w + 1)c^{p_1+p_2}} \right]^{1/q} \quad (3)$$

A fairly wide range of values of p_1 , p_2 , σ and q fit the data well because of variability in the data. We assumed that the neural response to coherence was best fit by a linear coherence-response function ($q = 1$), since it has been shown that the response of many macaque MT neurons to the preferred direction of motion (using a random dot stimulus very similar to the one used on our experiment) increases approximately linearly with coherence (Britten, Shadlen, Newsome, & Movshon, 1993). Though almost half of MT neurons showed significant nonlinearities, approximately half these cells showed compressive nonlinearities while the other half showed accelerating nonlinearities; thus the modal response seemed to be linear with coherence.

The variables describing the contrast function were also fixed ($p_1 = 0.02$, $p_2 = 1.49$, and $\sigma = 2.2$) based on a pooled estimate of the neuronal contrast response function from 80 neurons in MT (Sclar, Maunsell, &

Lennie, 1990; Thiele, Dobkins, & Albright, 2000). These parameters define an accelerating contrast-response function at contrasts below $\sim 2\%$ and a compressive function at higher contrasts. Psychophysical measurement of reaction times for detecting the onset of motion of sinusoidal gratings found that the effects of contrast could be modeled using similar contrast response functions as those described by Sclar et al. (Burr & Corsale, 2001). The fit of the model when variables p_1 , p_2 , σ and q were constrained in this way was nearly as good as when they were allowed to vary freely.

The variable r was fit simultaneously for every angular separation between the direction of the two dot fields (each value of δ). We allowed a different value of w for each angular separation of the coherent dot fields (δ). We constrained w to be 1 when $\delta = 0$; with zero angular separation both of the two fields have an equal influence on the detecting mechanism.

4.1. Model results

The model fit curves are shown with solid colored lines in Fig. 3. Since only w was allowed to vary with δ , the shape of the iso-performance functions remains constant, and each curve is simply shifted towards or away from the origin. This is demonstrated in panel H, which overlays the model predictions for each value of δ on a single plot.

Because a single variable w describes the shift of the curves as a function of angular separation of the dot fields, δ , our model contains within it the assumption that bandwidth does not change with either contrast or coherence. If bandwidth varied with either contrast or coherence, we would see a change in shape of the coherence vs. contrast iso-performance function as δ varied. For example, if bandwidths were narrower for low coherence/high contrast stimuli than for high coherence/low contrast stimuli we would expect the slope in log-log co-ordinates to be steeper for $\delta > 0^\circ$ than for $\delta = 0^\circ$. This was not observable in our data.

These values of w can be considered as describing the bandwidth of motion mechanisms. Shown in Fig. 4 are values of w from the best fit to the data plotted as a function of δ in polar coordinates. As described above, we set $w = 1$ for $\delta = 0^\circ$; a value of 1 therefore implies perfect summation between the two dot fields (Eq. (1)). As can be seen from Fig. 4, we see a decrease in summation as δ increases, up to values of $\delta = 90^\circ$, as would be expected. However, as δ increases beyond 90° , summation begins to *increase*. This increase in summation as the angular difference between the two dot fields increases beyond 90° has been reported in other studies in the literature as increased sensitivity to “shearing” or relative motion (see Section 5).

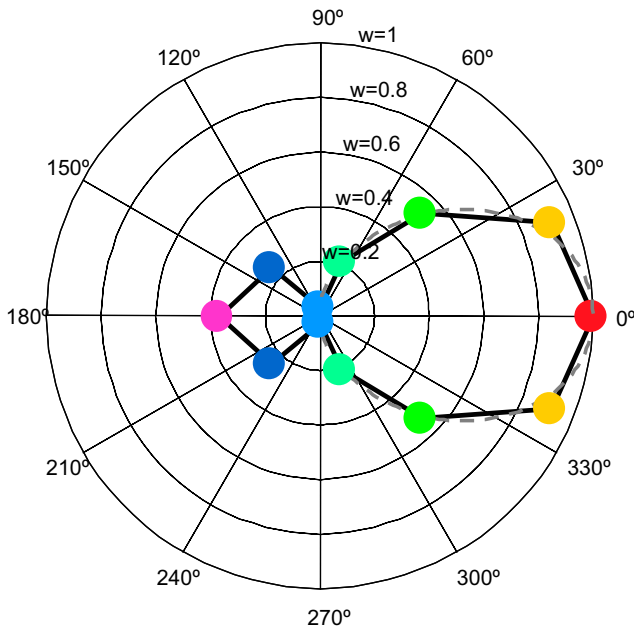


Fig. 4. The solid line shows w as a function of δ in polar co-ordinates. The angle represents δ and varies between 0° and 360° . The radius represents the value of w and varies between 0 and 1. Given the assumptions of our model, this figure represents the bandwidth of the directionally tuned mechanisms mediating performance in our task. The dashed line represents the best fitting Gaussian for $\delta < 90^\circ$.

There are small systematic deviations from the model: for example thresholds for high coherence/low contrast stimuli (coherence $>50\%$, contrast $<3\%$) tended to be slightly higher than predicted by the model across all values of δ . This may be due to there being a fixed contrast threshold of around 3%, regardless of the coherence of the stimulus or the directional difference between the two dot fields. At rms contrasts around 3% the stimulus subjectively appeared to be near detection threshold (i.e. it was difficult to see the dots regardless of their motion), thus it is possible that this asymptote represents limits in the ability of observers to detect the presence of the dots below a certain contrast (possibly a limitation at a stage of processing before MT?).

Gaussian functions, $w = w_{90^\circ} + e^{(-0.5 \times \delta^2 / \sigma^2)}$, were fitted to the function describing w as a function of δ_{0-90° in order to estimate bandwidth (Raymond, 1993; Watamaniuk et al., 1989; Williams, Tweten, & Sekuler, 1991). w_{90° is the weight at $\delta = 90^\circ$ and σ is the standard deviation of the best-fitting Gaussian. The mid-point of the Gaussian was set at $\delta = 0^\circ$, and $w_{\delta > 90^\circ}$ were excluded. We used a maximum likelihood fitting procedure to find the best value of σ . The resulting Gaussian function is plotted with a dashed gray line in Fig. 4. The tuning function of w is well described by a Gaussian with a bandwidth (width at half-height) of 89.8° . As discussed below, this estimate is very similar to those found in many other psychophysical and physiological studies.

Another prediction of this model is that it should be possible to predict iso-performance curves for other performance thresholds (e.g. 60% or 95% performance) simply by allowing r to vary and keeping all other parameters fixed. As described above, R is the response of the mechanism as a function of contrast, coherence and δ , and $R = r$ is the response required for a given performance level. We therefore fit iso-performance curves for other performance thresholds (between 55% and 95% correct). The parameters p_1 , p_2 , q and σ were fixed as described above, and w was fixed using the simultaneous fit values obtained for 75% correct iso-performance curves. We then allowed only r to vary to fit other performance levels. The fits for 55%, 60%, 70%, 80%, 90% and 95% iso-performance curves for $\delta = 0^\circ$ are shown in Fig. 5. Fits for other values of δ were similar.

The model fits performance thresholds above 70% reasonably well, with r as the only free variable. The fact

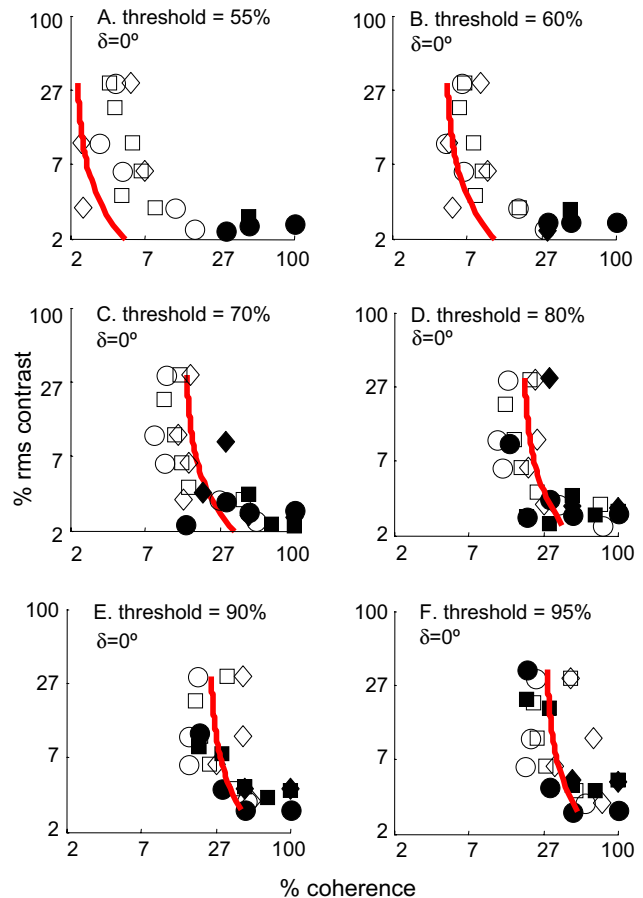


Fig. 5. Iso-performance plots for 55%, 60%, 70%, 80%, 90% and 95% correct performance for $\delta = 0^\circ$. Once again, the x-axis represents contrast, the y-axis represents coherence and each point represents the particular conjunction of contrast and coherence that resulted in the correct performance plotted in the graph. The fit from our model is shown using red curves. The shape of the curve does not change with performance threshold, but shifts away from the origin as the performance threshold increases.

that the shape of the model curves needs not vary to adequately fit these other performance thresholds demonstrates that bandwidth does not vary as the direction of motion of the stimuli becomes more apparent. However the model does not fit performance thresholds below 60% well. As mentioned earlier, some of the deviation between the model and the data may be due to there being a fixed contrast threshold: once the contrast of the dots is below $\sim 3\%$, observers' had trouble seeing the dots themselves: thresholds may have depended upon the visibility of the dots rather than the coherence of the stimulus or the directional difference between the two dot fields. At low performance thresholds this low contrast asymptote becomes more apparent.

It is also very likely that the parameters of our model underestimate the acceleration in the contrast response function for low contrasts. Greater acceleration at low contrasts would have two effects on our model: first, isoperformance curves would be shifted further away from the origin for low performance levels, thus providing better fits than those currently provided by the model. Second, model fits would bend to asymptote along the x -axis more sharply. This would also improve the fit of the model by reducing the mismatch between model predictions and data for high coherence/low contrast stimuli.

5. Discussion

The results of our study demonstrate that the tuning bandwidths of motion mechanisms are relatively constant across a reasonably broad range of stimulus contrasts and coherences.

We suspect that our model is the simplest that could be used to explain the data. While the model has six degrees of freedom, four of these (p_1 , p_2 , σ , q) are used to describe the known contrast and coherence response functions of MT+ neurons. Of the two remaining variables, r was used to predict different performance levels, and w was allowed to vary to predict the effects of direction. Given how well w was fit by a Gaussian function it seems plausible that $w_{\delta \leq 90}$ could have been constrained to a Gaussian function without significant loss of predictive power. However, despite the model's constraints, it is relatively successful at predicting performance across a broad range of contrasts, coherences and directional differences.

We did see a systematic deviation between our model and the data for high coherences and low contrasts—observers' performance is better than the model would predict. This deviation from the model occurs for all values of δ , and thus cannot be modeled by assuming that bandwidth changes with either contrast or coherence. However, the deviation is what would be predicted

if we had underestimated the accelerating response of motion mechanisms to low contrast.

Our model assumes that a given magnitude of response $R = r$ (in the mechanism best tuned to the stimulus) produces a fixed threshold of performance in terms of percent correct. Thus our model did not incorporate probability summation, but rather assumed that performance is simply mediated by the most sensitive mechanism reaching a certain response threshold. However it is plausible to assume that when $\delta = 0$, only half as many neurons would be tuned to the single direction of motion present in the stimulus, compared to when $\delta > 0$ and two directions of motion are present. The effect of probability summation is therefore to produce better observer performance for $\delta > 0$, compared to $\delta = 0$. We found that incorporating probability summation into our model narrowed estimated bandwidth slightly (sensitivity fell off more sharply with δ and there was a small amount of inhibition between orthogonal dot directions) but did not change model fits significantly.

5.1. Psychophysical measurements of bandwidth

Many psychophysical studies of directional tuning for motion mechanisms report bandwidths (width at half-height) of approximately 120° – 150° , values that are considerably broader than the 90° bandwidth we report in the present study (Ball & Sekuler, 1979, 1980; Ball et al., 1983; Levinson & Sekuler, 1975, 1976). However, two psychophysical studies do report tuning bandwidths similar to ours. In a selective adaptation paradigm, Raymond (1993) obtained estimates of tuning bandwidths by measuring coherence thresholds (for high contrast dots) before and after adaptation and found bandwidths of approximately 80° . Also, Levinson and Sekuler (1980) found bandwidths of $\sim 90^\circ$ for a contrast detection task (subjects increased the contrast until the test dots were barely visible) following adaptation.

These discrepancies in estimated bandwidth across different psychophysical studies may depend whether or not stimuli are suprathreshold. Performance at threshold is thought to be based on the responses of only the most sensitive mechanisms, while performance for stimuli above threshold is thought to involve a broader range of mechanisms (including those tuned for directions *close* to the stimulus direction of motion), which might result in wider estimates of bandwidth for tasks using suprathreshold stimuli (Graham, 1989; Raymond, 1993). For example, studies of reaction time (Ball & Sekuler, 1979; Levinson & Sekuler, 1980), and perceived direction of motion after adaptation (Levinson & Sekuler, 1976) used suprathreshold stimuli and observed relatively broad tuning bandwidths while studies measuring coherence thresholds have tended to find narrower directional tuning (Raymond, 1993).

Estimates of directional bandwidth may also broaden for very low contrast stimuli. We observed a fixed threshold of about 3% contrast regardless of stimulus coherence or the directional difference between the two dot fields. At very low contrasts the ability to detect the dots, rather than the ability to detect coherent motion, may play a role in limiting performance. This would have the effect of flattening the apparent bandwidth.

5.2. Neurophysiological measurements of bandwidth

Directional tuning bandwidths have been reported to vary between visual area, with MT direction selective neurons reported to have tuning bandwidths of $\sim 80^\circ$ (Albright, 1984; Britten & Newsome, 1998; Dubner & Zeki, 1971; Felleman & Kaas, 1984; Rodman & Albright, 1987). In contrast, direction selective units in area V1 have a mean direction tuning bandwidth of about 40° (De Valois, Yund, & Hepler, 1982; Schiller, Finlay, & Volman, 1976). The bandwidth of 90° that we report here is therefore remarkably similar to the neurophysiological bandwidths found for MT neurons. Although, MST, STPa, and VIP units exhibit similar direction tuning bandwidths to MT units (Gabel, Misslisch, Gielen, & Duysens, 2002; Oram, Perrett, & Hietanen, 1993) MT is the first stage in the cortical hierarchy that exhibits physiological tuning bandwidths similar to the psychophysical bandwidths. It therefore seems plausible that performance on our task was mediated by MT rather than V1 or higher motion areas (Mikami, Newsome, & Wurtz, 1986a, 1986b; Newsome, Britten, & Movshon, 1989; Newsome & Pare, 1988).

5.3. Invariance of bandwidth across contrast and coherence: evidence for contrast (and coherence) normalization

The data in the present study demonstrate roughly invariant directional tuning across a reasonably broad range of contrasts and coherences. The responses of direction selective neurons (Sclar et al., 1990) are known to saturate at high contrasts. Without some process of normalization, this contrast saturation would result in broader tuning functions at higher contrasts.

Similar invariance with contrast has been described for orientation tuning (Sclar & Freeman, 1982; Skottun et al., 1987). This has been attributed to a combination of half-rectification and normalization nonlinearities (Carandini, Heeger, & Movshon, 1997; Ferster & Miller, 2000; Geisler & Albrecht, 1997; Heeger, 1992, 1993). Normalization could result from either feed-forward signals combined with push–pull inhibition (Ferster & Miller, 2000) or feedback intracortical connections (Adorjan, Levitt, Lund, & Obermayer, 1999; Ben-Yishai, Bar-Or, & Sompolinsky, 1995; Ben-Yishai, Hansel, & Sompolinsky, 1997; Hansel & Sompolinsky, 1996; Hansel & van Vreeswijk, 2002; Somers, Nelson, &

Sur, 1995). Analogous models predict that direction tuning should also be invariant with contrast (Dean, Hess, & Tolhurst, 1980; Heeger, 1992, 1993). For example, the responses of cat simple cells to counter-phase and drifting grating patterns as a function of contrast (Albrecht & Geisler, 1991) have been described using a model (linear spatiotemporal receptive-field structure, a compressive contrast-responses and half-wave rectification) analogous to those that predict invariance of orientation bandwidth with contrast. According to these contrast normalization models, directional tuning bandwidth should be constant with contrasts, in spite of the limited dynamic response range and steep slope of the contrast-response function.

Although our model does not include an explicit normalization term, it models contrast-response and coherence-response functions with the parameters p_1 , p_2 , σ and q , and assumes that directional selectivity does not change as a function of either contrast or coherence. This is the same as assuming the existence of contrast (and possibly coherence) normalization. The good fit of the model to the data thus provides further support for the notion of contrast normalization within the visual cortex.

5.4. Shearing motion

Slightly surprisingly, the results of our study revealed greater summation between the two moving dot fields when they were separated by an angular difference of 180° than when they were separated by 90° (see Figs. 3, 4). This effect implies heightened sensitivity to the “shearing” or “relative” motion present in the 180° condition than to orthogonal (90°) motion. Similar results have already been reported by a variety of previous psychophysical studies (Krauskopf & Li, 1999; Lu & Sperling, 1995; Moller & Hurlbert, 1996; Nakayama, 1981; Seiffert & Cavanagh, 1998; Snowden, 1992; Tsujimura & Zaidi, 2002) showing greater sensitivity for shearing than orthogonal motion. Neurons sensitive to relative motion have also been described in cats within the superior colliculus (Mandl, 1985) and area 17 (Burns, Gassanov, & Webb, 1972); in the owl monkey in area MT (Allman, Miezin, & McGuinness, 1985), the superior colliculus (Bender & Davidson, 1986) and area V2 (Orban, Gulyas, & Spileers, 1987); and in macaque MT (Tanaka et al., 1986). It has also been found that discrete lesions to area MT of the rhesus monkey lowered performance on a shear detection task (Siegel & Andersen, 1986). It is postulated that specialized center-surround neural mechanisms may account for sensitivity to shearing motion (Kim & Wilson, 1997; Sachtler & Zaidi, 1995).

Our model (see Fig. 4) implies either that individual neurons have a bimodal direction tuning function, or that there is a bimodal distribution of neuronal tuning.

Evidence from other studies suggests that the neurons mediating sensitivity to shear may be different mechanisms than those mediating sensitivity to uniform motion. For example, relative motion detectors can be selectively adapted (Shioiri, Ono, & Sato, 2002) and around 20% of humans show a selective lack of sensitivity to shearing motion (Richards & Lieberman, 1982).

To conclude, we find that at intermediate coherences and contrast values there is a tradeoff between contrast and coherence, such that increasing either contrast or coherence improves performance. However the bandwidth of directionally selective mechanisms seems to change remarkably little as a function of either contrast or coherence. This relative invariance of directional tuning bandwidth across a range of contrasts and coherence levels is consistent with models of contrast normalization.

Acknowledgements

Supported by NIH Grant EY12153 (KRD).

References

- Adorjan, P., Levitt, J. B., Lund, J. S., & Obermayer, K. (1999). A model for the intracortical origin of orientation preference and tuning in macaque striate cortex. *Visual Neuroscience*, 16(2), 303–318.
- Albrecht, D. G., & Geisler, W. S. (1991). Motion selectivity and the contrast-response function of simple cells in the visual cortex. *Visual Neuroscience*, 7(6), 531–546.
- Albright, T. D. (1984). Direction and orientation selectivity of neurons in visual area MT of the macaque. *Journal of Neurophysiology*, 52(6), 1106–1130.
- Allman, J., Miezin, F., & McGuinness, E. (1985). Direction- and velocity-specific responses from beyond the classical receptive field in the middle temporal visual area (MT). *Perception*, 14(2), 105–126.
- Ball, K., & Sekuler, R. (1979). Masking of motion by broadband and filtered directional noise. *Perception and Psychophysics*, 26(3), 206–214.
- Ball, K., & Sekuler, R. (1980). Models of stimulus uncertainty in motion perception. *Psychological Review*, 87(5), 435–469.
- Ball, K., Sekuler, R., & Machamer, J. (1983). Detection and identification of moving targets. *Vision Research*, 23(3), 229–238.
- Bender, D. B., & Davidson, R. M. (1986). Global visual processing in the monkey superior colliculus. *Brain Research*, 381(2), 372–375.
- Ben-Yishai, R., Bar-Or, R. L., & Sompolinsky, H. (1995). Theory of orientation tuning in visual cortex. *Proceedings of the National Academy of Sciences USA*, 92(9), 3844–3848.
- Ben-Yishai, R., Hansel, D., & Sompolinsky, H. (1997). Traveling waves and the processing of weakly tuned inputs in a cortical network module. *Journal of Computational Neuroscience*, 4(1), 57–77.
- Britten, K. H., & Newsome, W. T. (1998). Tuning bandwidths for near-threshold stimuli in area MT. *Journal of Neurophysiology*, 80(2), 762–770.
- Britten, K. H., Shadlen, M. N., Newsome, W. T., & Movshon, J. A. (1993). Responses of neurons in macaque MT to stochastic motion signals. *Visual Neuroscience*, 10(6), 1157–1169.
- Burns, B. D., Gassanov, U., & Webb, A. C. (1972). Responses of neurons in the cat's visual cerebral cortex to relative movement of patterns. *Journal of Physiology*, 226(1), 133–151.
- Burr, D. C., & Corsale, B. (2001). Dependency of reaction times to motion onset on luminance and chromatic contrast. *Vision Research*, 41, 1039–1048.
- Carandini, M., Heeger, D. J., & Movshon, J. A. (1997). Linearity and normalization in simple cells of the macaque primary visual cortex. *Journal of Neuroscience*, 17(21), 8621–8644.
- De Valois, R. L., Yund, E. W., & Hepler, N. (1982). The orientation and direction selectivity of cells in macaque visual cortex. *Vision Research*, 22(5), 531–544.
- Dean, A. F., Hess, R. F., & Tolhurst, D. J. (1980). Divisive inhibition involved in directional selectivity. *Journal of Physiology*, 308, 84P.
- Dubner, R., & Zeki, S. M. (1971). Response properties and receptive fields of cells in an anatomically defined region of the superior temporal sulcus in the monkey. *Brain Research*, 35(2), 528–532.
- Felleman, D. J., & Kaas, J. H. (1984). Receptive-field properties of neurons in middle temporal visual area (MT) of owl monkeys. *Journal of Neurophysiology*, 52(3), 488–513.
- Ferster, D., & Miller, K. D. (2000). Neural mechanisms of orientation selectivity in the visual cortex. *Annual Review of Neuroscience*, 23, 441–471.
- Gabel, S. F., Misslisch, H., Gielen, C. C., & Duysens, J. (2002). Responses of neurons in area VIP to self-induced and external visual motion. *Experimental Brain Research*, 147(4), 520–528.
- Geisler, W. S., & Albrecht, D. G. (1997). Visual cortex neurons in monkeys and cats: detection, discrimination, and identification. *Visual Neuroscience*, 14(5), 897–919.
- Georgeson, M. A., & Scott-Samuel, N. E. (2000). Spatial resolution and receptive field height of motion sensors in human vision. *Vision Research*, 40(7), 745–758.
- Graham, N. (1989). Visual pattern analyzers. *Oxford psychology* (vol. 16). Oxford University Press: Oxford.
- Hansel, D., & Sompolinsky, H. (1996). Chaos and synchrony in a model of a hypercolumn in visual cortex. *Journal of Computational Neuroscience*, 3(1), 7–34.
- Hansel, D., & van Vreeswijk, C. (2002). How noise contributes to contrast invariance of orientation tuning in cat visual cortex. *Journal of Neuroscience*, 22(12), 5118–5128.
- Heeger, D. J. (1992). Normalization of cell responses in cat striate cortex. *Visual Neuroscience*, 9(2), 181–197.
- Heeger, D. J. (1993). Modeling simple-cell direction selectivity with normalized, half-squared, linear operators. *Journal of Neurophysiology*, 70(5), 1885–1898.
- Kim, J., & Wilson, H. R. (1997). Motion integration over space: interaction of the center and surround motion. *Vision Research*, 37(8), 991–1005.
- Krauskopf, J., & Li, X. (1999). Effect of contrast on detection of motion of chromatic and luminance targets: Retina-relative and object-relative movement. *Vision Research*, 39(20), 3346–3350.
- Kukkonen, H., Rovamo, J., Tiippana, K., & Nasanen, R. (1993). Michelson contrast, RMS contrast and energy of various spatial stimuli at threshold. *Vision Research*, 33(10), 1431–1436.
- Levinson, E., & Sekuler, R. (1975). The independence of channels in human vision selective for direction of movement. *Journal of Physiology*, 250(2), 347–366.
- Levinson, E., & Sekuler, R. (1976). Adaptation alters perceived direction of motion. *Vision Research*, 16(7), 779–781.
- Levinson, E., & Sekuler, R. (1980). A two-dimensional analysis of direction-specific adaptation. *Vision Research*, 20(2), 103–107.
- Lu, Z. L., & Sperling, G. (1995). The functional architecture of human visual motion perception. *Vision Research*, 35(19), 2697–2722.
- Mandl, G. (1985). Responses of visual cells in cat superior colliculus to relative pattern movement. *Vision Research*, 25(2), 267–281.
- Meese, T. S., & Harris, M. G. (2001). Broad direction bandwidths for complex motion mechanisms. *Vision Research*, 41(15), 1901–1914.

- Mikami, A., Newsome, W. T., & Wurtz, R. H. (1986a). Motion selectivity in macaque visual cortex. I. Mechanisms of direction and speed selectivity in extrastriate area MT. *Journal of Neurophysiology*, 55(6), 1308–1327.
- Mikami, A., Newsome, W. T., & Wurtz, R. H. (1986b). Motion selectivity in macaque visual cortex. II. Spatiotemporal range of directional interactions in MT and V1. *Journal of Neurophysiology*, 55(6), 1328–1339.
- Moller, P., & Hurlbert, A. C. (1996). Psychophysical evidence for fast region-based segmentation processes in motion and color. *Proceedings of the National Academy of Sciences USA*, 93(14), 7421–7426.
- Morrone, M. C., Burr, D. C., & Vaina, L. M. (1995). Two stages of visual processing for radial and circular motion. *Nature*, 376(6540), 507–509.
- Moulden, B., Kingdom, F., & Gatley, L. F. (1990). The standard deviation of luminance as a metric for contrast in random-dot images. *Perception*, 19(1), 79–101.
- Nakayama, K. (1981). Differential motion hyperacuity under conditions of common image motion. *Vision Research*, 21(10), 1475–1482.
- Newsome, W. T., Britten, K. H., & Movshon, J. A. (1989). Neuronal correlates of a perceptual decision. *Nature*, 341(6237), 52–54.
- Newsome, W. T., & Pare, E. B. (1988). A selective impairment of motion perception following lesions of the middle temporal visual area (MT). *Journal of Neuroscience*, 8(6), 2201–2211.
- Oram, M. W., Perrett, D. I., & Hietanen, J. K. (1993). Directional tuning of motion-sensitive cells in the anterior superior temporal polysensory area of the macaque. *Experimental Brain Research*, 97(2), 274–294.
- Orban, G. A., Gulyas, B., & Spileers, W. (1987). A moving noise background modulates responses to moving bars of monkey V2 cells but not monkey V1 cells. *Investigative Ophthalmology Visual Science Supplement*, 28, 197.
- Raymond, J. E. (1993). Movement direction analysers: independence and bandwidth. *Vision Research*, 33(5–6), 767–775.
- Raymond, J. E. (1994). Directional anisotropy of motion sensitivity across the visual field. *Vision Research*, 34(8), 1029–1037.
- Richards, W., & Lieberman, H. R. (1982). Velocity blindness during shearing motion. *Vision Research*, 22(1), 97–100.
- Rodman, H. R., & Albright, T. D. (1987). Coding of visual stimulus velocity in area MT of the macaque. *Vision Research*, 27(12), 2035–2048.
- Sachtler, W. L., & Zaidi, Q. (1995). Visual processing of motion boundaries. *Vision Research*, 35(6), 807–826.
- Scase, M. O., Braddick, O. J., & Raymond, J. E. (1996). What is noise for the motion system? *Vision Research*, 36(16), 2579–2586.
- Schiller, P. H., Finlay, B. L., & Volman, S. F. (1976). Quantitative studies of single-cell properties in monkey striate cortex. II. Orientation specificity and ocular dominance. *Journal of Neurophysiology*, 39(6), 1320–1333.
- Sclar, G., & Freeman, R. D. (1982). Orientation selectivity in the cat's striate cortex is invariant with stimulus contrast. *Experimental Brain Research*, 46(3), 457–461.
- Sclar, G., Maunsell, J. H., & Lennie, P. (1990). Coding of image contrast in central visual pathways of the macaque monkey. *Vision Research*, 30(1), 1–10.
- Seiffert, A. E., & Cavanagh, P. (1998). Position displacement, not velocity, is the cue to motion detection of second-order stimuli. *Vision Research*, 38(22), 3569–3582.
- Shioiri, S., Ono, H., & Sato, T. (2002). Adaptation to relative and uniform motion. *Journal of Optical Society of America A—Optics Image Science and Vision*, 19(8), 1465–1474.
- Siegel, R. M., & Andersen, R. A. (1986). Motion deficits following ibotenic acid lesions of the middle temporal area (MT) in the behaving rhesus monkey. *Society for Neuroscience Abstracts*, 12, 1183.
- Skottun, B. C., Bradley, A., Sclar, G., Ohzawa, I., & Freeman, R. D. (1987). The effects of contrast on visual orientation and spatial frequency discrimination: a comparison of single cells and behavior. *Journal of Neurophysiology*, 57(3), 773–786.
- Snowden, R. J. (1992). Sensitivity to relative and absolute motion. *Perception*, 21(5), 563–568.
- Somers, D. C., Nelson, S. B., & Sur, M. (1995). An emergent model of orientation selectivity in cat visual cortical simple cells. *Journal of Neuroscience*, 15(8), 5448–5465.
- Tanaka, K., Hikosaka, K., Saito, H., Yukie, M., Fukada, Y., & Iwai, E. (1986). Analysis of local and wide-field movements in the superior temporal visual areas of the macaque monkey. *Journal of Neuroscience*, 6(1), 134–144.
- Thiele, A., Dobkins, K. R., & Albright, T. D. (2000). Neural correlates of contrast detection at threshold. *Neuron*, 26(3), 715–724.
- Tsujimura, S.-I., & Zaidi, Q. (2002). Similarities between visual processing of shear and uniform motion. *Vision Research*, 42, 3005–3017.
- van Hateren, J. H. (1990). Directional tuning curves, elementary movement detectors, and the estimation of the direction of visual movement. *Vision Research*, 30(4), 603–614.
- Watamaniuk, S. N., Sekuler, R., & Williams, D. W. (1989). Direction perception in complex dynamic displays: the integration of direction information. *Vision Research*, 29(1), 47–59.
- Williams, D., Tweten, S., & Sekuler, R. (1991). Using metamers to explore motion perception. *Vision Research*, 31(2), 275–286.